InAs/InP(100) QD waveguide photodetectors for a monolithically integrated optical coherence tomography system around 1.7 μm

Y. Jiao, B.W. Tilma, J. Kotani, R. Nötzel, M.K. Smit, E.A.J.M. Bente
COBRA Research Institute, Eindhoven University of Technology
Eindhoven, The Netherlands
y.jiao@tue.nl

***Abstract*—InAs/InP(100) quantum dot (QD) waveguide photodetectors are presented in this paper. The devices are fabricated using the layer stack of semiconductor optical amplifiers (SOAs) and are compatible with the active-passive integration technology. The characterization and simulation on the devices have shown good potential to be used in a monolithically integrated swept-source optical coherence tomography (SS-OCT) system in 1.6 to 1.8 μm wavelength range.**

Keywords-quantum dot; photodetector; optical coherence tomography; integrated optoelectronics

I. INTRODUCTION

The swept-source optical coherence tomography (SS-OCT) in 1.6 to 1.8 μm wavelength range is of great interest in medical imaging. The swept-source scheme provides higher sensitivity [1] while the long wavelength offers deeper imaging depth [2]. Two main components are required to open up OCT imaging in an SS-OCT system in this long wavelength range. The first is a swept laser source. In previous work [3], we have developed an experimental monolithically integrated tunable laser around the 1.7 μm wavelength region using InAs/InP(100) quantum dots (QDs) as its optical amplifiers. The feasibility of this laser had been demonstrated in a free-space Michelson interferometer setup. A suitable photodetector is thus the second main component that is essential to realize the potential for OCT imaging in the 1.6 to 1.8 μm range. Such detectors are not readily available commercially. In this paper we present InAs/InP(100) QD waveguide photodetectors which meet all the requirements for application in an SS-OCT system in the 1.6 to 1.8 μm wavelength range. The main advantage is that the presented photodetectors can be monolithically integrated with our swept laser and other components.

II. DEVICES AND MEASUREMENTS

The QD waveguide photodetectors are realized by applying a reverse-bias voltage on a shallowly etched ridge waveguide QD semiconductor optical amplifier (QD-SOA). The QD-SOA structure is fabricated using a technology that is fully compatible with the active-passive optical integration scheme at our research institute [4]. As can be seen in Fig. 1, the layer stack of the QD photodetector is identical to that of the QD-SOAs which were used in our swept laser. This opens up a way of further integration of all active and passive components in a SS-OCT system. The fabricated two chips (with different total lengths) consist of 26 devices each with different device lengths.

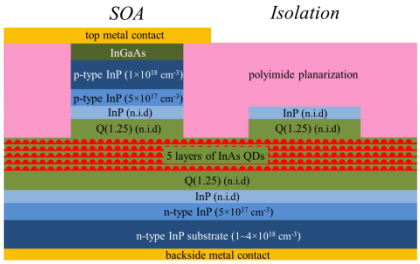

Figure 1. The cross-section structure of the QD-SOA section and isolation section.

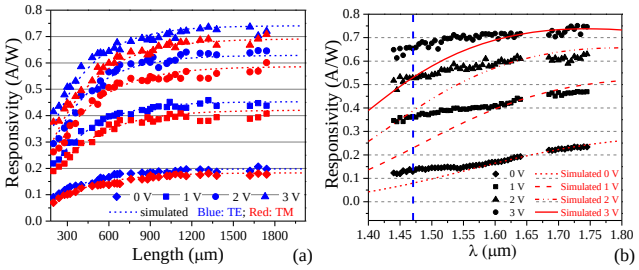

Figure 2. (a) The responsivities of 32 devices with different lengths at a wavelength of 1640 nm. (b) The spectral responses of a 960 μm-long device under different reverse-bias voltages for TE polarization.

Several properties of the photodetectors have been measured to demonstrate the feasibility of their use in the monolithically integrated SS-OCT system in 1.6 to 1.8 μm wavelength range. The measurements on the dark current lead to a conclusion that a sufficiently low dark current (< 30 nA) can be achieved by choosing the appropriate device length (< 1000 μm) and bias voltage (< 3 V). The responsivities as a function of length of the waveguide and bias voltages have also been measured as shown in Fig. 2(a). It is clear from the figure that the responsivity increases with the device length and after reaching a certain length (around 950 μm), almost all the photons are absorbed. It also can be seen that the responsivity of the QD photodetector can reach as high as 0.7 A/W which is more than sufficient for the SS-OCT application. The measured

spectral response of a device with a 960 μm length is shown in Fig. 2(b). It is clear in Fig. 2(a) and (b) that the responsivity of the photodetector increases dramatically with the reverse-bias voltage. The device shows a flat response over a whole 300 nm wavelength range which well satisfies the requirement for the SS-OCT application in 1.6 to 1.8 μm wavelength range.

The electrical signal bandwidth of the photodetectors is determined by measuring the photocurrents under a modulated optical input. The measurement is performed on several devices with different lengths and under several bias voltages. For a device with a length of 200 μm and a bias voltage of 2 V, the 3 dB bandwidth can reach 83 MHz, which is adequate for the OCT application.

III. Simulations

A modified rate equation model based of a QD-SOA model [4] is applied for the simulation of photodetection with current extraction. An equivalent circuit model is used to analyze the factors that limit the bandwidth of the devices.

Since we used identical QD active material and layer stack for the photodetector as for QD-SOA, the QD rate equation model and several of the parameters used in [4] were slightly modified to simulate the behavior of the photo-absorption of the QDs. The major modification from [4] is the change from current injection to current extraction. Another modification is that the multiple photon groups used for representing different wavelength components in the gain spectra is reduced to only one photon group which represents a single wavelength as in the measurements. The advantage of this modified model is that only one major parameter (carrier extraction rate from wetting layer to SCH layer) is adjusted to match the simulation with the measured data for one particular value of the reverse-bias voltage while all the other parameters for QD-SOA keep unchanged.

Simulations on the length-dependent responsivities are shown in Fig. 2(a) in dashed curves. As can be seen in the figure, the simulation results match very well with the measured data. Simulations for the spectral behavior of the photodetectors are also performed as shown in Fig. 2(b) in red curves. It can be seen in the figure that for wavelengths longer than 1.6 μm, the simulation matches well with the measured spectrum. But for the shorter wavelengths below 1.6 μm, there is a clear deviation between simulation and measurement. The absorption coefficient of the QDs in the shorter wavelength region is underestimated. One of the reasons can be the exclusion of contributions from higher-order excited states in the QDs. Such states would not show up in the ASE spectra in forward bias, but can play a role in absorption. Another reason which is more probable is the exclusion of contribution from the wetting layer. The energy level of the WL corresponds to a wavelength of 1.47 μm [4] and is indicated as a blue line in Fig. 2(b). This wavelength locates in the wavelength region where a clear deviation occurs.

The QD waveguide photodetectors can also be modeled using an equivalent circuit method [5]. The theoretical 3 dB bandwidth can be calculated by translating the photodetectors and connecting electronics into the equivalent circuit. By matching the simulated 3 dB bandwidth with the measured one, the value of probe pad capacitance C_p and the voltage dependency of junction capacitance C_{pd} of the diode can be determined as shown in Fig. 3. As C_p does not change as voltage, it keeps a relatively high value (as high as 46 pF). This is mainly due to the large area of the metal contact used in our devices. It can also be seen that there is a significant improvement on C_{pd} as the bias voltage increases. It is mainly due to the expansion of the depletion region as the voltage increases.

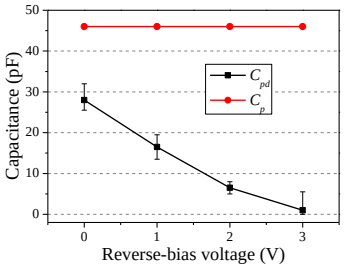

Figure 3. The determined values of C_{pd} and C_p under different reverse-bias voltages. The error bars indicate the variability of C_{pd} when the ±5 % relative deviation of the bandwidth values used in the calculation is considered.

IV. Conclusion

In this paper we have presented the QD waveguide photodetectors and have shown them to meet all requirements for application in SS-OCT in the 1.6 to 1.8 μm wavelength range. Both rate equation model and equivalent circuit model have well explained the behaviors of the photodetectors. The devices have shown good potential to be used in a monolithically integrated long-wavelength SS-OCT system.

Acknowledgment

The authors thank the support from the BrainBridge project, China Scholarship Council (CSC) and the NRC Photonics grant.

References

[1] M. Choma, M. Sarunic, C. Yang, and J. Izatt, "Sensitivity advantage of swept source and Fourier domain optical coherence tomography," *Opt. Express*, vol. 11, pp. 2183-2189, 2003.

[2] V. M. Kodach, J. Kalkman, D. J. Faber, and T. G. van Leeuwen, "Quantitative comparison of the OCT imaging depth at 1300 nm and 1600 nm," Biomed. Opt. Express, vol. 1, pp. 176-185, 2010.

[3] B. W. Tilma, Y. Jiao, J. Kotani, B. Smalbrugge, H. P. M. M. Ambrosius, P. J. Thijs, X. J. M. Leijtens, R. Notzel, M. K. Smit, and E. A. J. M. Bente, "Integrated Tunable Quantum-Dot Laser for Optical Coherence Tomography in the 1.7 μm Wavelength Region," IEEE J. Quant. Electron., vol. 48, pp. 87-98, 2012.

[4] B. W. Tilma, M. S. Tahvili, J. Kotani, R. Notzel, M. K. Smit, and E. A. J. M. Bente, "Measurement and analysis of optical gain spectra in 1.6 to 1.8 μm InAs/InP (100) quantum-dot amplifiers," Opt. Quant. Electron., vol. 41, pp. 735-749, 2009.

[5] H. Jiang and P. K. L. Yu, "Equivalent circuit analysis of harmonic distortions in photodiode," IEEE Photon. Technol. Lett., vol. 10, pp. 1608-1610, 1998.